



Research Article

Simulink Methods to Simulate the COVID-19 Outbreak Using Fractional Order Models

Srilekha R ^{id}, Parthiban V* ^{id}

School of Advanced Sciences, Vellore Institute of Technology, Chennai, India
Email: parthiban.v@vit.ac.in

Received: 1 March 2023; **Revised:** 4 May 2023; **Accepted:** 15 July 2023

Abstract: The objective of this work is to solve a coronavirus transmission model using Simulink, a platform for model-based design that facilitates simulation and design at the system level. The simulation is divided into two sections: the first deals with setting up the parameters, and the second deals with computing the fractional derivatives. The fundamental susceptible-infected-removed (SIR), susceptible-exposed-infected-recovered (SEIR), susceptible-exposed-infected-isolated-recovered (SEIQR), and susceptible-exposed-infected-asymptotically infected-recovered-reservoir (SEIARM) models were used in this study. An effective, quick, easy, and visually appealing method is used to simulate pandemic outbreaks. To accurately follow the progress of the infection, we contrast the simulation findings with those acquired by MATLAB code. The applications can be used for research projects and as a teaching tool.

Keywords: fractional mathematical model, fuzzy fractional mathematical model, coronavirus, Simulink

MSC: 34A08, 93-04, 92B99, 00A71

1. Introduction

The first case of the novel coronavirus appeared in China, in Wuhan city, which the World Health Organisation (WHO) identified as SARS-CoV-2 and COVID-19. The WHO labelled this infectious disease a pandemic on March 11, 2020. This lethal illness spreads quickly and is very contagious, passing from person to person. Human-to-human transmission of the virus occurs through nasal discharge and saliva droplets when an infected person coughs or sneezes, which is how the infection spreads. Through contaminated hands that touch the mouth, nose, and eyes, the virus can enter the body. The virus spread quickly around the world, forming numerous large-scale clusters [1].

Using computer simulations based on an epidemic's mathematical model is one technique to forecast the epidemic's dynamic spread. There is a Python code called CHIME (COVID-19 Hospital Impact Model for Epidemics) developed for use in hospitals. Several analytical methods have been put out in the literature to model the pandemic, such as the susceptible-infected-removed (SIR) model [2], susceptible-exposed-infected-recovered (SEIR) [3], susceptible-infected-recovered-dead (SIRD) [4], and many more. The need for creating an open-source computer program that can do a time-domain simulation of the dynamic spread of the virus was studied by [5] for integer order. There are a few articles that explain the numerical methods for solving the COVID-19 outbreak [6]. On top of that, there is an increasing urge to study the behaviour of the dynamics of the COVID-19 model when its integer order is replaced

by fractional order. Recently, academicians' interest in studying fractional calculus has increased enormously. This is because fractional calculus can more effectively describe and process the preservation and inheritance properties of different structures than integer-order models. The physical basis of the fractional operators with different memories that describe the behaviour of systems with memory or long-range dependence, where the response of the system depends on past values of the input or state variables over a certain range of time or space, is achieved with fractional calculus. These operators are used to model a wide range of real-world phenomena, such as anomalous diffusion, visco-elastic materials, and signal processing in communication systems. The physical basis of fractional operators with different memories can be understood in terms of the concept of fractional differentiation, which generalises the classical integer-order differentiation to non-integer orders. In classical calculus, integer-order derivatives describe the rate of change of a function with respect to an independent variable, such as time or space. Fractional derivatives, on the other hand, describe the rate of change of a function with respect to a non-integer order, which introduces the concept of memory or persistence in the system's response. Many applications of fractional calculus were included in various research articles [7-10]. Therefore, utilising various mathematical methodologies, researchers extended the classical calculus to the fractional order via fractional order modelling. In order to deal with differential equations in both fractional and classical order, a number of approaches, including the Adomian decomposition method, homotopy and variation techniques, and the Fourier transform method [11-14], have been developed.

An instructional software that visualises the mathematical model of virus spread as a block diagram is the easiest way to understand epidemic disease spread. Various infections spread by mathematical models have been studied by many authors [15-18]. MATLAB/Simulink is one of the most popular platforms for examining a system's dynamic behaviour. It has been utilised by numerous academicians in a variety of time-domain simulations of dynamic systems. Differential equations (DEs) can be used to mathematically model a dynamic system, such as the COVID-19 spread. The key difficulty with such a simulation is estimating the model's parameters, such as infection and recovery rates. Anyhow, we can estimate the parameter value because we know the initial value.

Here, it is important to know about the various models and how they are developed for studying their dynamic behaviour. The basic model of all epidemic diseases is the SIR model (Figure 1), wherein S is the susceptible population and I and R are the infected and recovered, respectively, which are the compartments that represent each stage of epidemic disease. The susceptible population is the percentage of people who are susceptible to the disease at time (t) , denoted by $S(t)$. After some time, the susceptible population will move to the infected compartment $I(t)$. Infected populations are those people who are infected by the virus and are ready to spread the disease to other individuals. Recovered populations are those who are recovered from the disease and would have developed immunity to that particular virus; thus, this population will again go back to the susceptible population, giving rise to another model called SIRS (Figure 2), but in this paper, we will study simulating the SIR model and other models like SIRD, susceptible-exposed-infected-isolated-recovered (SEIQR), susceptible-exposed-infected-asymptotically infected-recovered-reservoir (SEIARM), and $SEII_AQI_HI_cR$, which are extensions of the basic SIR model. Next, it becomes crucial to know about the parameters used in the construction of the model. When we have the S, I, and R populations, it is mandatory to know about the rate at which they spread. In this paper, γ is the rate of transmission of the virus from the S to I population and ϱ is the rate at which infected become recovered are discussed.

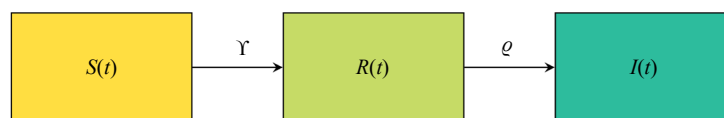


Figure 1. Block diagram for SIR model

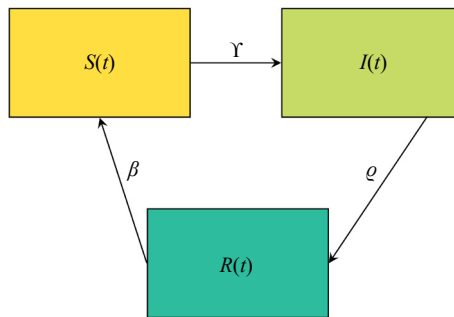


Figure 2. Block diagram for SIRS mode

This study proposes a generalised method to track and estimate the viral spread globally in a simple, effective, and visually appealing manner using Simulink for the SIR, SIRD, SEIQR, and SEIARM. The fractional operator has been used in a number of disciplines, including engineering, physics, and chemistry. Because ordinary differential operators have typically been ineffective in predicting the memory and heredity properties of materials and processes, by using fractional order operators, they can be thoroughly discussed with real, appropriate remarks. Furthermore, since Reimann-Liouville, Caputo, and Atangana-Baleanu type fractional operators provided the most notable definitions among the fractional differential operators, Caputo derivatives have primarily been used to treat biological models of infectious disease. This is because of its initial condition independence, consistency with physical interpretation, empirical validation in providing a good fit to experimental data or observed behaviours of diseases, and its compatibility with the integer order derivative. For example, the study of the motion of a beam on an internally bent nanowire using a Caputo derivative is done in this article [19]. Disease modelling in oncolytic virology is dealt with in the article [20]. [21] deals with the analysis of climatic change using the Caputo fractional derivative. Authors in [22] and [23] analysed the bibliography on artificial neural networks using fractional derivatives and how fractional derivatives are extensively used in image processing, respectively. The authors of [24-26] found out the applications of fractional derivatives in the Caputo sense in optics, chemical reactor theory, and the dynamics of the alkali-silica reaction, respectively. Our article deals with simulating the epidemic model of non-integer or fractional order using Simulink.

The significance of our proposed work are as follows:

- Accurate simulation: Fractional-order models are more accurate in describing the complex behaviour of infectious diseases like COVID-19 compared to traditional integer-order models. Simulink's ability to simulate such models accurately allows for more accurate predictions of the spread of the virus and the impact of interventions.
- Flexibility: Simulink provides a flexible environment for building and testing models of different complexity levels. This flexibility is especially important for COVID-19 simulations, where there are many uncertainties and changing conditions.
- Visualisation: Simulink provides a graphical interface that allows users to visualise the behaviour of the model over time. This is important for understanding the impact of interventions and communicating the results of the simulation to stakeholders.
- Optimisation: Simulink provides tools for optimising the parameters of the model to match real-world data. This can help improve the accuracy of the simulation and make it more useful for decision-making.

Overall, Simulink methods to simulate the COVID-19 outbreak using fractional order models are significant because they provide a powerful tool for understanding the dynamics of the pandemic and making informed decisions about interventions to mitigate its impact. The paper is structured as follows: A brief explanation of the COVID-19 pandemic sickness is provided in Section 1, along with the evolution of the fractional calculus. Fractional calculus fundamentals are covered in Section 2. A detailed explanation of the Simulink model and simulation is presented in Section 3. The graphical method used to determine the model's approximative system solution is presented in this section, along with the educational value of Simulink. Section 4 contains the article's conclusion.

2. Preliminaries

Throughout this paper we will be denoting C to be the fractional order.

Definition 1. The Riemann-Liouville fractional derivative of order $C \geq 0$ is defined as

$$D^C f(t) = \frac{1}{\Gamma(n-C)} \left(\frac{d}{dt} \right)^n \int_0^t (t-s)^{n-C-1} f(s) ds, t \geq 0,$$

where $\Gamma(\cdot)$ is the Euler gamma function.

Definition 2. The Caputo fractional derivative of order $C \geq 0$ with $(n-1) \leq C \leq n, n \in \mathbb{N}$, for a suitable function f is defined as

$${}^c D^C f(t) = \frac{1}{\Gamma(n-C)} \int_0^t (t-s)^{n-C-1} f^{(n)}(s) ds.$$

Definition 3. A fuzzy number is a mapping such as $u: \mathbb{R} \rightarrow [0,1]$, where u is the membership function satisfying the following conditions:

- u is upper semi continuous.
- u is fuzzy convex (i.e.)

$$u((\lambda x) + (1-\lambda)y) \geq \min\{u(x), u(y)\}, \forall x, y \in \mathbb{R}, \lambda \in [0,1]$$

- u is normal (i.e.) $\forall x_0 \in \mathbb{R}$ with $u(x_0) = 1$.
- $\text{supp } u = \{x \in \mathbb{R} | u(x) > 0\}$ is the support of the u , and its closure $cl(\text{supp } u)$ is compact.

Definition 4. By the definition of fuzzy number defined earlier it follows that the ι -cut is the crisp set $[u]^\iota$ that contains all elements in \mathbb{R} such that the membership value of A is greater than or equal to α that is,

$$[u]^\iota = \{x \in \mathbb{R} : u(x) \geq \iota, \iota \in [0,1]\}$$

For a fuzzy number U , its ι -cuts are closed intervals in \mathbb{R} and we denote them by

$$[u]^\iota = [\underline{u}^\iota, \bar{u}^\iota]$$

We refer to \underline{u} and \bar{u} as the lower and upper bounds on u , respectively.

Definition 5. Let $f(t, r)$ be a fuzzy valued function and $[f(t; r)] = [f_-(t, r), \bar{f}(t, r)]$ for $r \in [0,1]$, $0 < C < 1$.

- If $f(t)$ is a Caputo-type fuzzy fractional differentiable function in first form, then

$${}^c D^C f(t) = \frac{1}{\Gamma(n-C)} \int_0^t (t-s)^{(n-C-1)} f^n_s ds.$$

- If $f(t)$ is a Caputo-type fuzzy fractional differentiable function in second form, then

$${}^c D^C f(t) = \frac{1}{\Gamma(n-C)} \int_0^t (t-s)^{(n-C-1)} \underline{f}^n_s ds.$$

3. Simulation example

Any dynamical system can be modelled with the help of Simulink, making use of the set of differential equations

in that system, thus making it doable for an epidemic system to be modelled and simulated using Simulink. Figure 3 shows the block that calculates each compartment in the model with accuracy for the various fractional orders we need. The toolbox that contains this block is the FOTF toolbox in MATLAB. The user needs to install the fractional order transfer function toolbox in order to solve any fractional-order problem in a dynamic system. In Figure 3, the fractional differentiator and fractional integrator blocks are given for reference for fractional order 0.3.

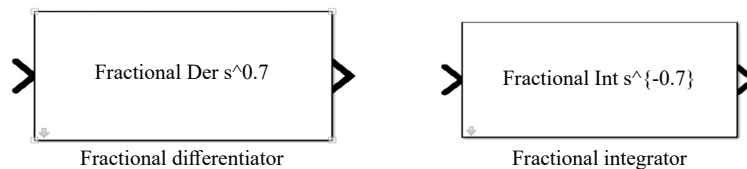


Figure 3. Fractional block in Simulink

3. Simulation of models such as SIR, SIRD, SEIQR, and SEIARM

3.1 SIR model

The SIR model is a classic compartmental model for predicting the progression of infectious disease. Its roots can be traced back to Kermack and McKendrick’s seminal work in the early twentieth century [27-29]. A simulation example is provided in Figure 4 to demonstrate how the problem is modelled in Simulink using the set of differential equations for the fractional orders 0.2, 0.4, and 0.6. In this model of the total population, there are three epidemiological classes: $S(t)$ (susceptible class), $I(t)$ (infected class), and $R(t)$ (recovered class). In the diagram, the blocks S, S1, and S2 are the right-hand side of the system (1) for the above-mentioned fractional orders. The initial conditions $S(0)$, $I(0)$, and $R(0)$ are to be provided in the integrator block, respectively. Here, we use the notation,

- Υ - infected rate
- ϱ - recovered rate

In order to solve the system, we use Simulink in our study.

$$\begin{cases} D^C S(t) = -\frac{\Upsilon \mathcal{J}(t)S(t)}{N} \\ D^C \mathcal{J}(t) = \frac{\Upsilon \mathcal{J}(t)S(t)}{N} - \varrho I(t) \\ D^C R(t) = \varrho \mathcal{J}(t) \end{cases} \quad (1)$$

correlated with initial conditions

$$\begin{aligned} S(0) &= S_0 \\ I(0) &= I_0, \\ R(0) &= R_0 \end{aligned}$$

The above-mentioned system’s Simulink block diagram is shown in Figure 4.

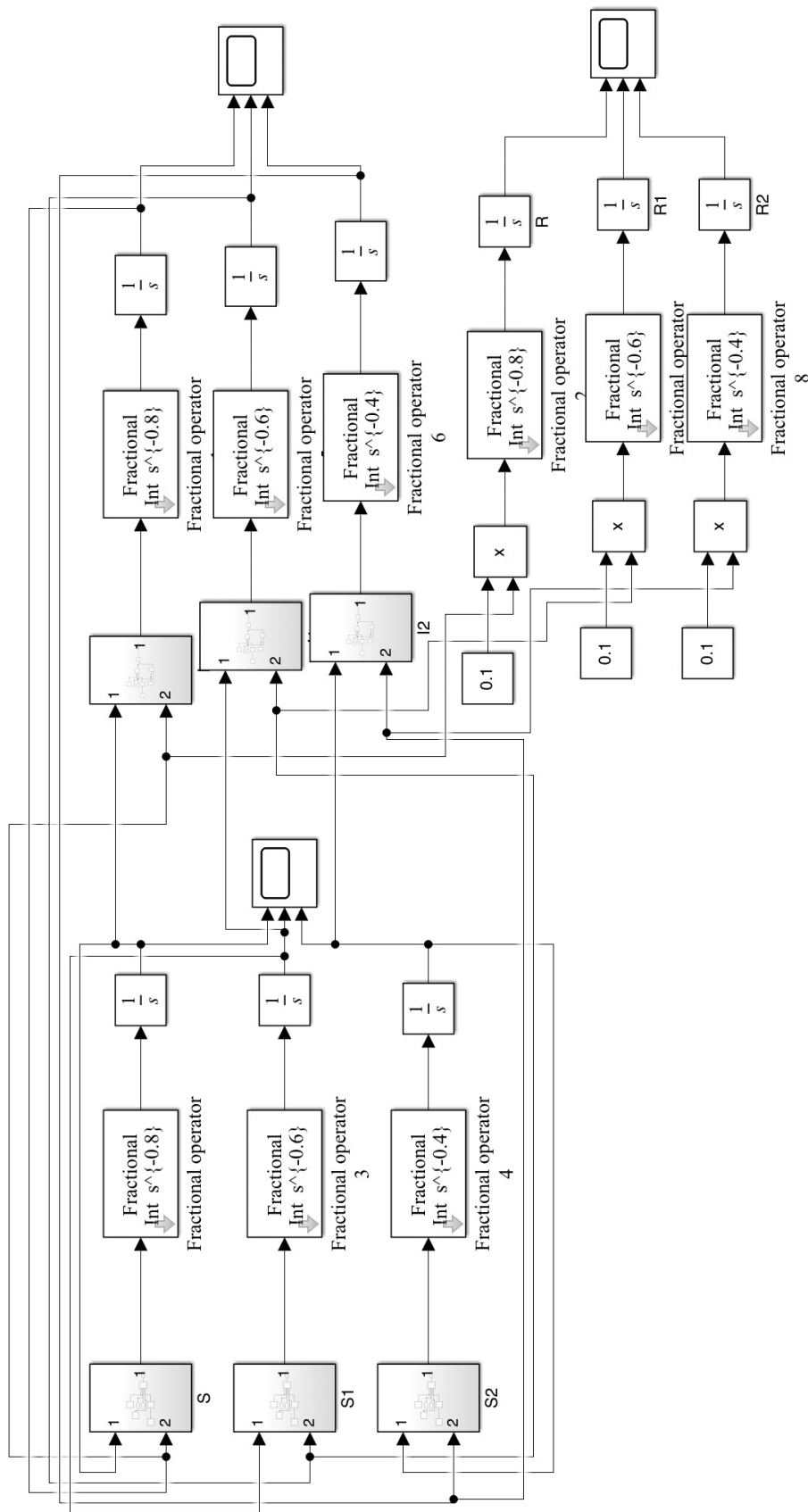


Figure 4. Block diagram of Simulink for equation (1)

This is where we acquire a lot of information on the model's dynamical behaviour. The numerical simulations of the Caputo model employing biological parameters are presented here. We used the Simulink graphical representation to identify the solution to the nonlinear model stated in equation (1) and generated graphical results based on parameters that are assumed to be variables. Various parameter values are used to study susceptible, infected, and recovered populations. As demonstrated in Figure 5(A), the number of susceptible individuals rises as the fractional order rate rises, whereas the number of infected people increases as the fractional order decreases, as shown in Figure 5(B), which makes sense because the susceptible population is transferred to compartment $I(t)$ following infection, resulting in an increase in that compartment. If C gets smaller, the recovered population drives ahead, as shown in Figure 5(C). The Caputo SIR model that is proposed is being utilised to better understand the behaviour of COVID-19, a terrible disease that has recently spread throughout the whole human community. The parameters were obtained from the paper [30].

The graph used to represent the dynamics of an infectious disease epidemic is the epidemic curve, which shows the number of new infections (or new cases) over time. The epidemic curve can provide insights into the rate of spread of the disease, the peak of the epidemic, and the decline in new infections as the epidemic subsides. The shape of the epidemic curve can vary depending on the parameters of the SIR model, such as the transmission rate and recovery rate, and the effectiveness of interventions, such as social distancing measures or vaccination campaigns.

The graphical results obtained from Simulink can be compared to those obtained by MATLAB code. See Figure 6 for reference. In this graph, the susceptible population is depicted in blue, whereas the infected and recovered populations are depicted in red and green, respectively, for the fractional order 0.6.

With regard to the parameter set, we investigate the time series behaviour of the mathematical model for susceptible, infected, and recovered. To illustrate the fluctuation in these variables, we use a 10-week time frame. Figures 5(A), 5(B), and 5(C) illustrate the rise and abrupt decline in the infected population as well as the sharp rise in the recovered population.

This can be explained by noting that, depending on the severity of the disorders being treated, the more infectious agents that are found, the higher the rate of recovery of those agents.

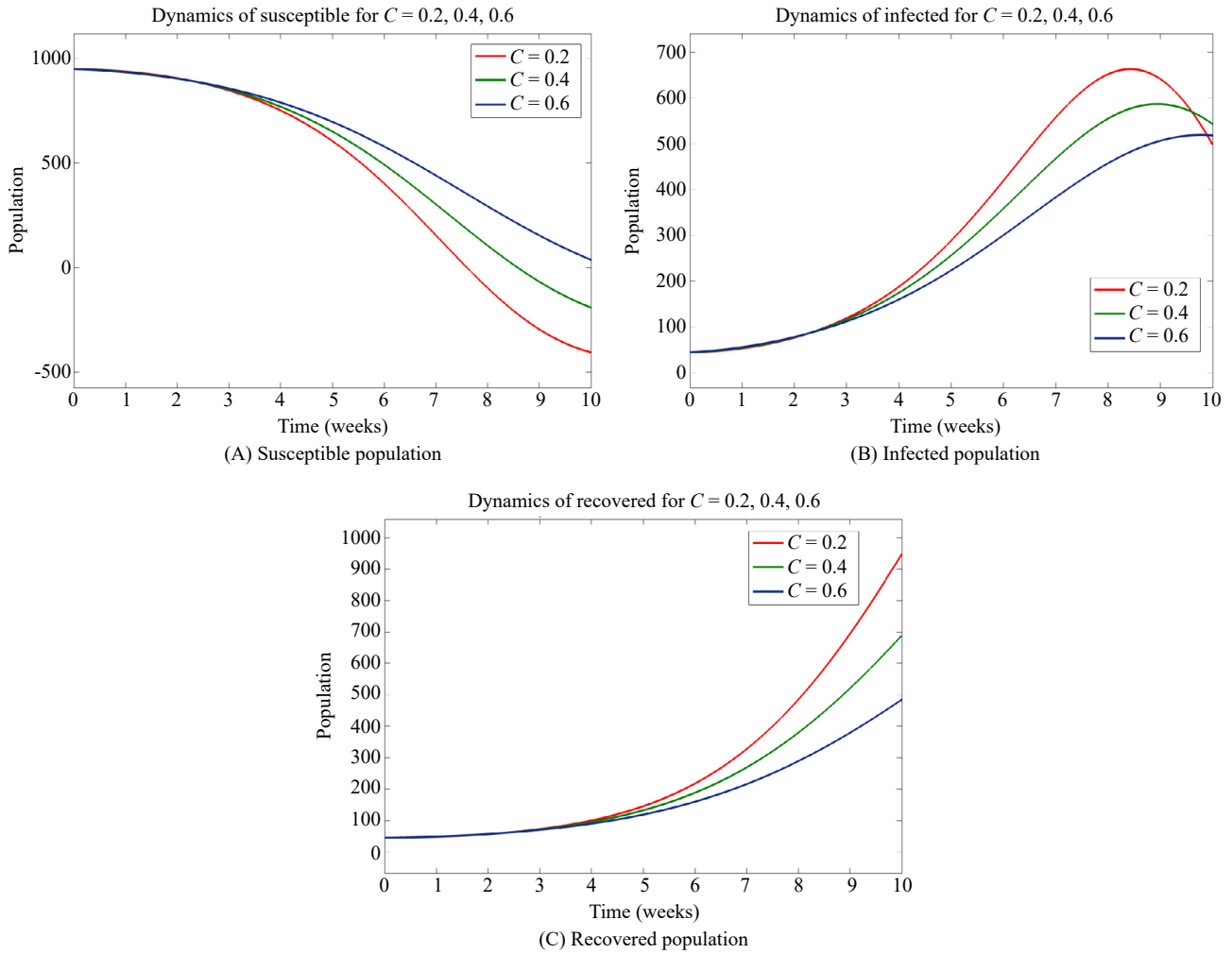


Figure 5. Dynamic behaviour of SIR model for $C = 0.2, 0.4,$ and 0.6

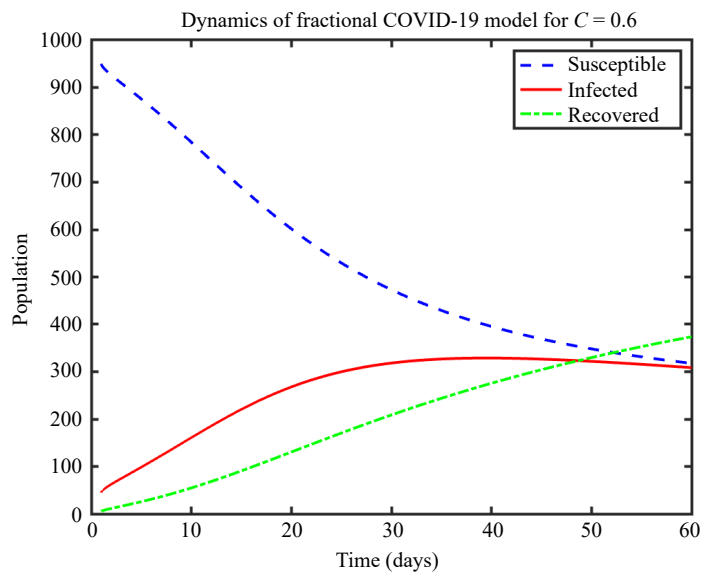


Figure 6. SIR model behaviour for $C = 0.6$

3.2 SIRD model

The SIR model discussed above is unable to provide data on infected and unrecovered dead individuals. The closed cases of infectious people who have passed away are not disclosed. The SIRD model can be created by including a death variable in the SIR model. This new SIRD compartmental model was first introduced by Hasan et al. [31] and later studied in [32-35].

The SIRD model is a mathematical model used in epidemiology to depict the link between susceptible cases, infected cases, recovered cases, and deceased cases in an epidemic-affected population. Here, $S(t)$ is the susceptible population, $I(t)$ is the infected population, $R(t)$ is the recovered population, and $D(t)$ is the deceased number. The fractional SIRD model accounts for mortality and is described by four fractional-order differential equations. The first equation represents the rate of vulnerable cases over time, the second equation represents the rate of infected cases over time, and the third equation represents the rate of recovered cases over time. The second equation shows the rate of infected cases as a function of time, while the third and fourth equations show the rate of recovered cases and deceased patients as functions of time, respectively.

The SIRD model's first two equations are nonlinear differential equations, whereas the model's final two equations are linear differential equations. In this case, we'll use the notation,

- Υ - infected rate
- ϱ - recovered rate
- ς - deceased rate

$$\begin{cases} \mathcal{D}_t^C [S(t)] = -\Upsilon \frac{S(t)\mathcal{J}(t)}{N} \\ \mathcal{D}_t^C [\mathcal{J}(t)] = -\Upsilon \frac{\mathcal{J}(t)S(t)}{N} - (\varrho + \varsigma)\mathcal{J}(t) \\ \mathcal{D}_t^C [R(t)] = \varrho\mathcal{J}(t) \\ \mathcal{D}_t^C [D(t)] = \varsigma\mathcal{J}(t) \end{cases} \quad (2)$$

correlated with the initial conditions,

$$S(0) = S_0, I(0) = I_0, R(0) = R_0, D(0) = D_0.$$

The above-mentioned system's Simulink block diagram is shown in Figure 7.

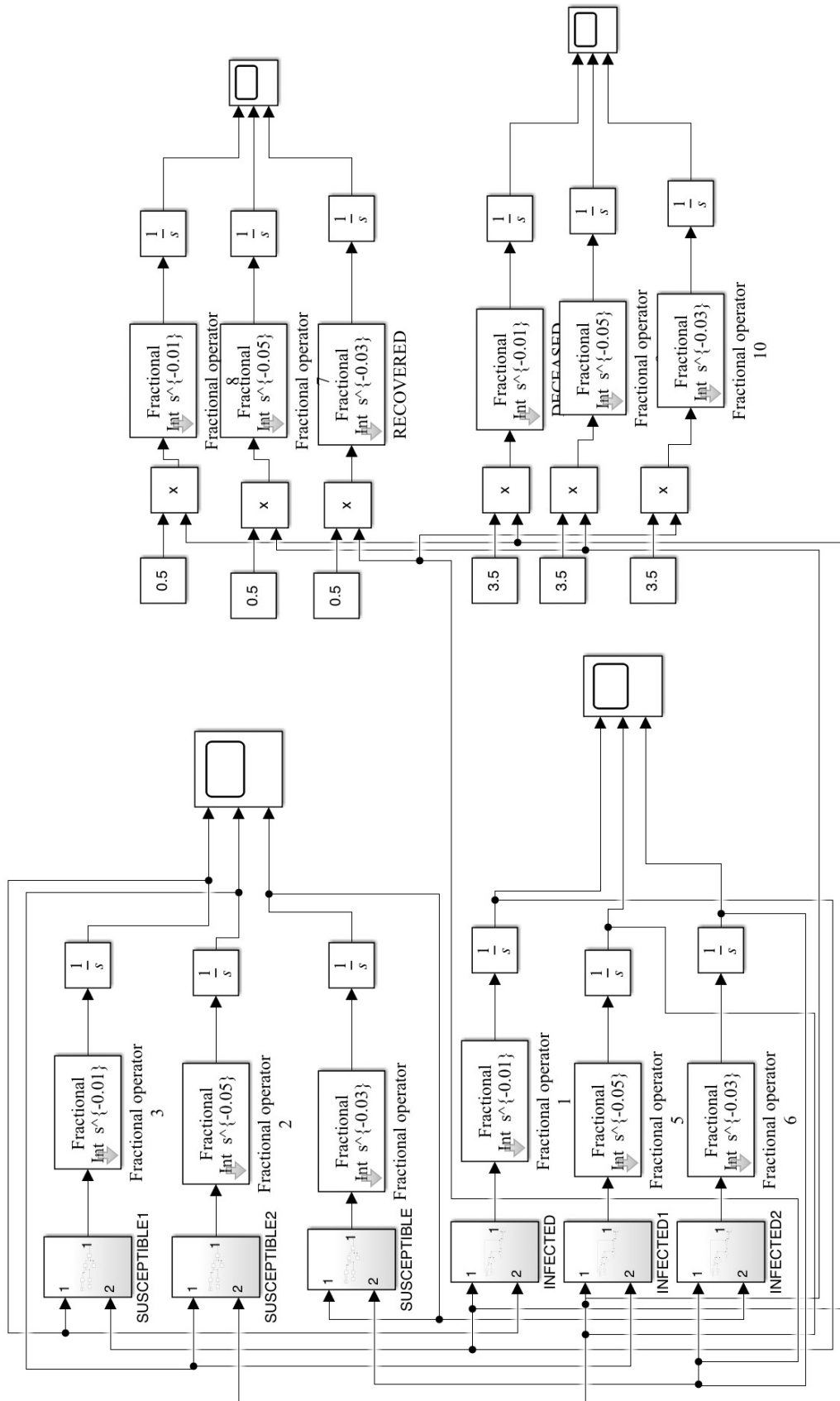


Figure 7. Block diagram of Simulink for equation (2)

We've supplied approximate solutions for several classes based on the data provided in [36] and corresponding to different fractional orders of 0.99, 0.97, and 0.95. We can observe that the population is presumed to be uninfected at first. The susceptible population continued to fall after the outbreak began, as can be seen in Figure 8(A). As a result, the population density of the infected class was rapidly increasing (Figure 8(B)) as they were exposed to infection. As a result of this growth, the death class increased (Figure 8(C)), and many people were able to rid themselves of the virus, contributing to a rise in the population that had recovered (Figure 8(D)). Furthermore, if the fractional order C approaches 1, all subsequent solutions will fulfil the integer-order solution. Since the fractional differential operator has a higher degree of freedom and gives a full geometric spectrum, we only used a few fractional orders to explore the model's dynamic behaviour.

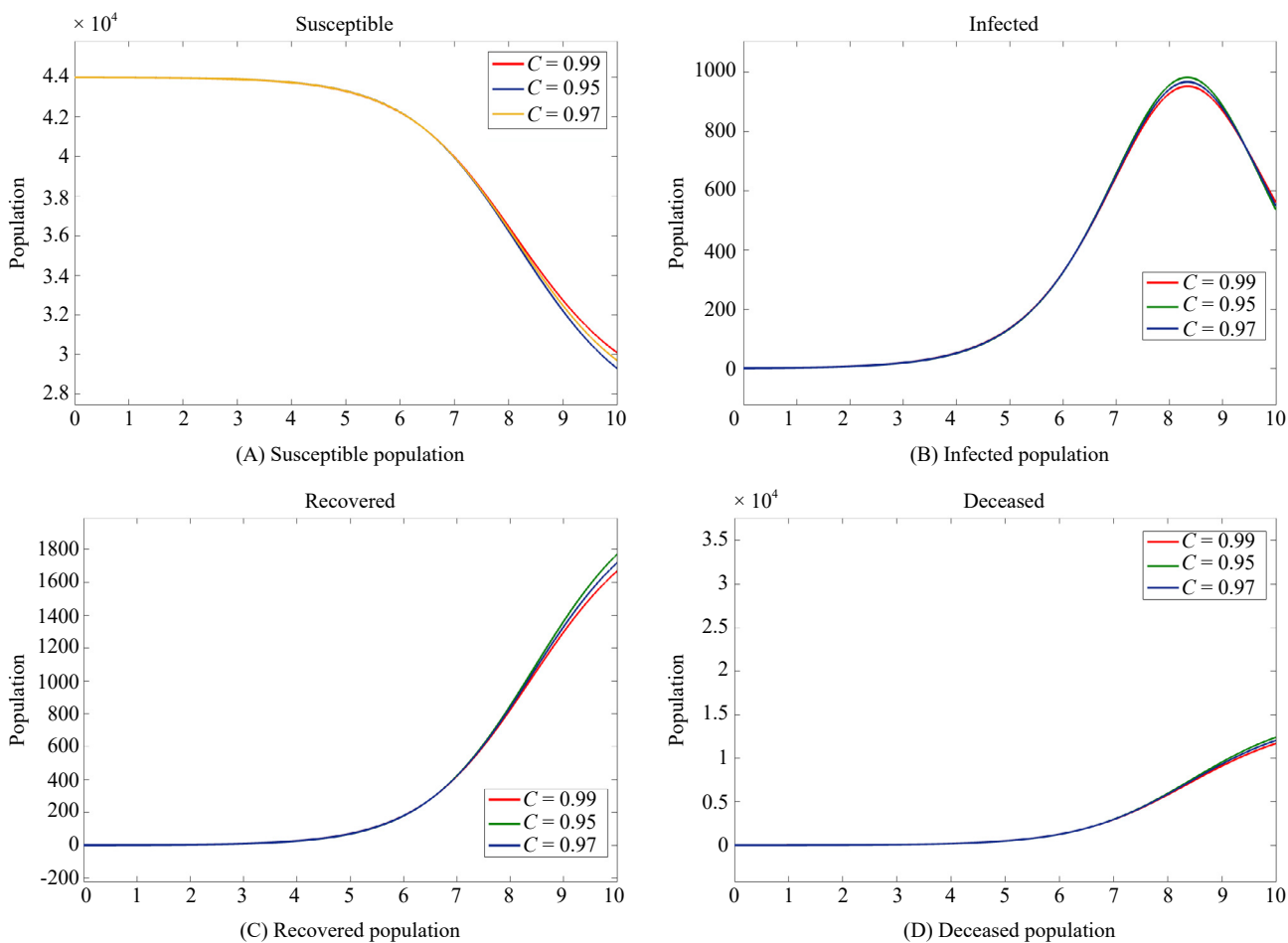


Figure 8. Dynamic behaviour of SIRD model for $C = 0.95, 0.97, \text{ and } 0.99$

We can see that the general public is first believed to be healthy (susceptible). The susceptible population decreased once the outbreak started, as depicted in Figure 8(A). Consequently, as they were exposed to infection, the infected class's population density was rapidly growing, as seen in Figure 8(B), until a certain stage. As a result of this surge, the mortality rate increased, and a large number of people were freed from the virus, which helped the population recover more quickly. The fractional order causes a difference in the rates of growth and decay. The speed of the process increases with the size of the order, and vice versa. Additionally, if the fractional order is less than 1, the following solutions always satisfy the integer-order solution. We just used a few fractional orders to examine the model's dynamic behaviours because the fractional differential operator has a higher degree of freedom and provides the entire geometric spectrum.

3.3 SEIQR model

We call our third model the SEIQR model since it contains susceptible, exposed, infected, isolated, and recovered. This new SEIQR compartmental model was first examined by Babaei et al. [37].

This mathematical model [38-40] deals with the interactions between the exposed and infected populations that are connected to the vulnerable population. In this model, $S(t)$ is the susceptible population, $E(t)$ is the exposed number of people, $I(t)$ is the infected population, $Q(t)$ is the isolated or quarantined population, and $R(t)$ is the recovered population. In this model, we assume that the disease death rate is incorporated into the natural death rate. When there are no signs of sickness, the exposed class moves at a set rate to the isolated class, but when symptoms arise, the exposed class proceeds to the infected class. In this case, we'll use the notation,

- η - recruitment rate
- Υ - the rate at which susceptible individuals become infected and exposed
- ϑ - the rate at which an exposed population becomes infected
- Ξ - the rate at which people who have been exposed to radiation become isolated
- \beth - infected people are added to isolated individuals at a rapid rate
- ϱ - recovered rate
- ς - deceased rate

$$\begin{cases} D_t^C S = \eta^C - \varsigma^C S - \nu^C S(\mathcal{E} + \mathcal{J}) \\ D_t^C \mathcal{E} = \nu^C S(\mathcal{E} + \mathcal{J}) - \vartheta^C \mathcal{E} - (\varsigma^C + \Xi^C) \mathcal{E} \\ D_t^C \mathcal{J} = \vartheta^C \mathcal{E} - \beth^C \mathcal{J} - \varsigma^C \mathcal{J} \\ D_t^C \mathcal{Q} = \xi^C \mathcal{E} + \beth^C \mathcal{J} - \varrho^C \mathcal{Q} - \varsigma^C \mathcal{Q} \\ D_t^C \mathcal{R} = \varrho^C \mathcal{Q}(t) - \varsigma^C \mathcal{R}(t) \end{cases} \quad (3)$$

The above-mentioned system's Simulink block diagram is shown in Figure 9.

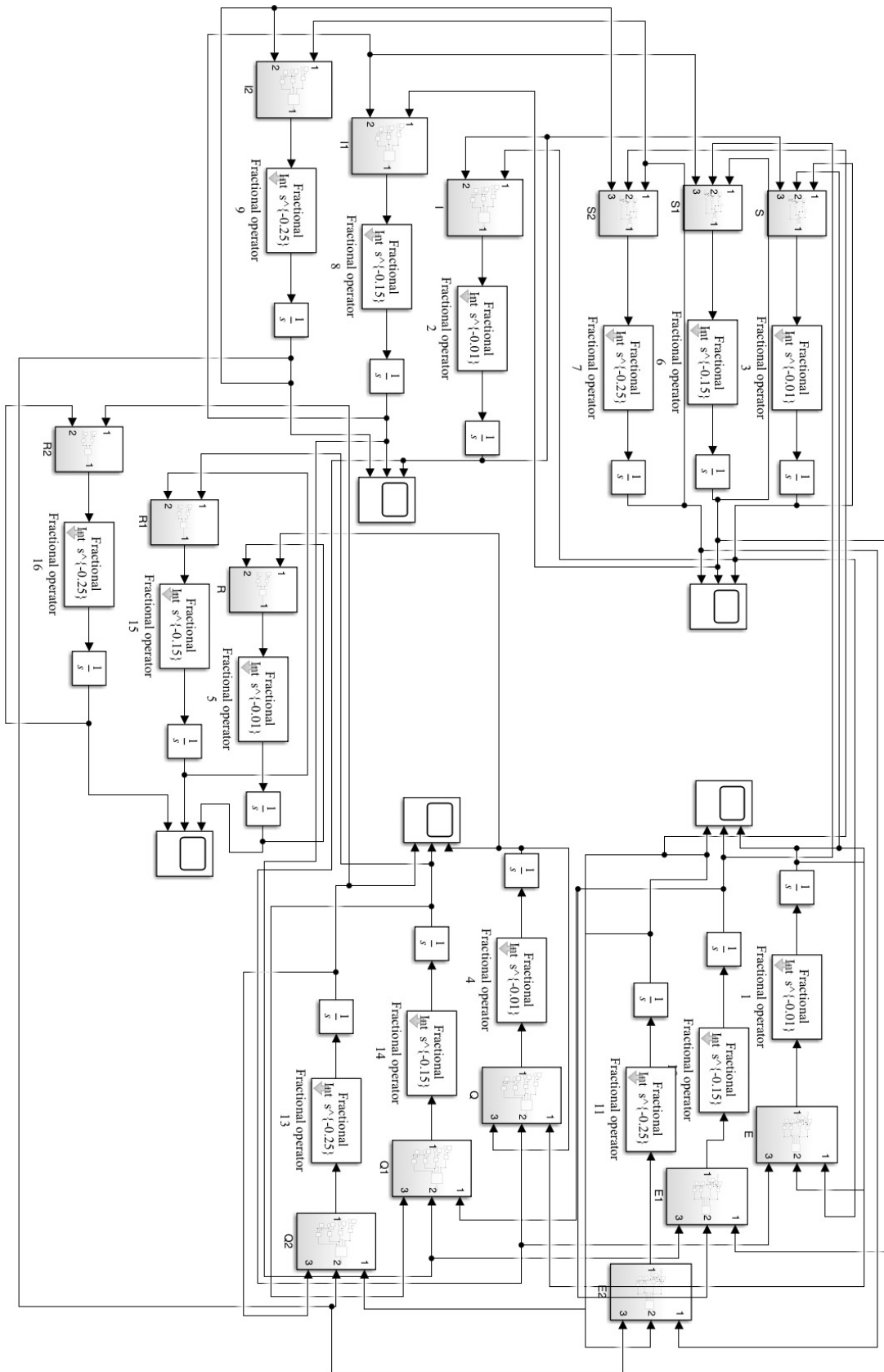


Figure 9. Block diagram of Simulink for equation (3)

With $T = 30$, we plot numerical solutions to the model. The results obtained using Simulink imply that the graph can accurately anticipate the behaviour of these variables in the region under study, as shown in the graphical results in Figures 10(A), 10(B), 10(C), 10(D), and 10(E). The approximate solutions are clearly dependent on the time fractional derivative C indefinitely. It is obvious that by reducing the step size, the efficiency of this method may be greatly improved.

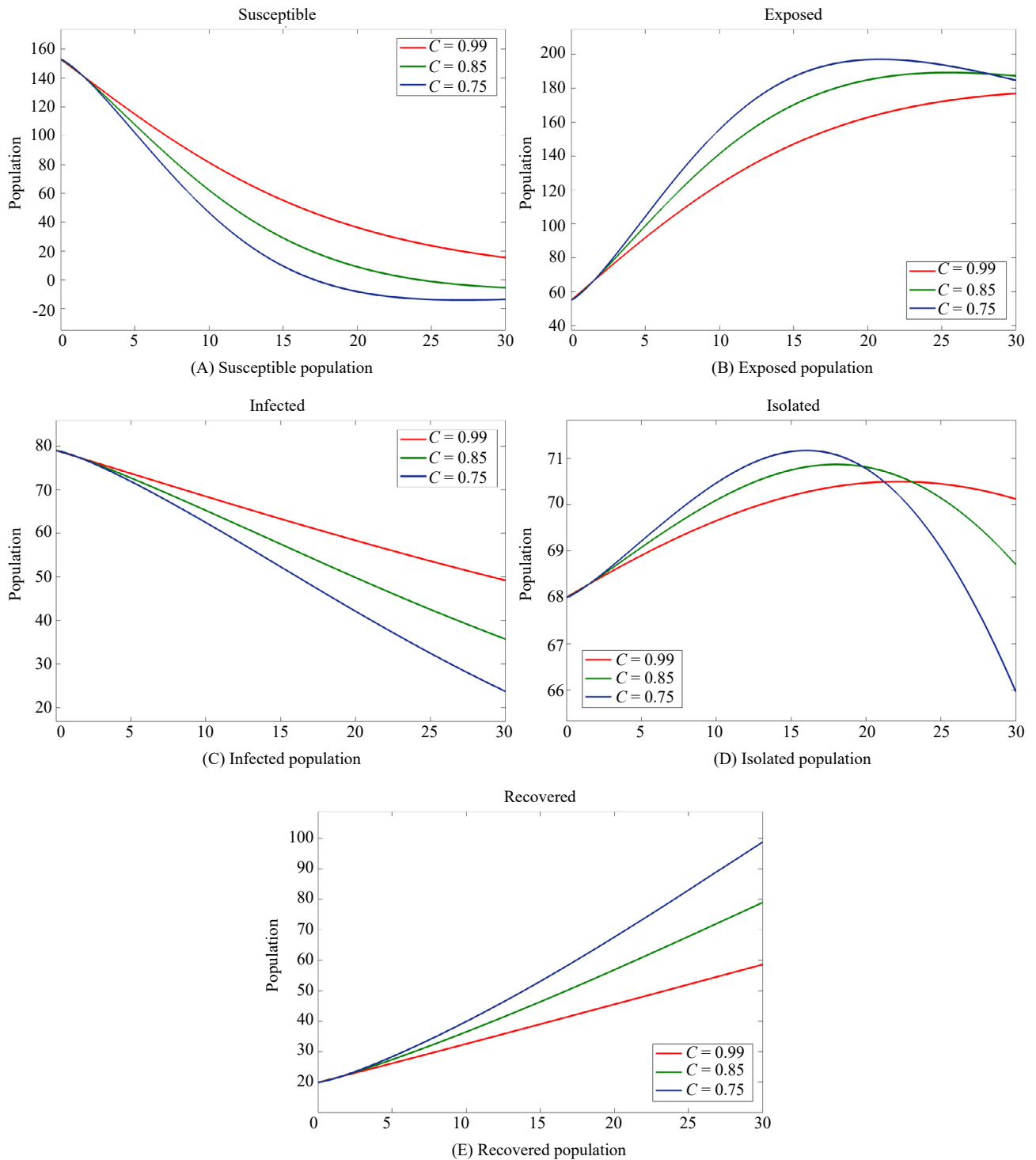


Figure 10. Dynamic behaviour of SEIQR model for $C = 0.75, 0.85,$ and 0.99

Initially, the susceptible population started to decline since the pandemic was growing exponentially, increasing the population of people exposed to the disease. By this time, control measures such as quarantine and isolation had started, which had a great effect on the control of COVID-19 spread, as we can clearly see from Figures 10(A), 10(B), 10(C), 10(D), and 10(E). We can very much infer from the simulation results that as there is isolation of the infected population, there is a considerable increase in the recovered population, which is helping the problem solve.

3.4 SEIARM model

The fourth model we will have for our study is the SEIARM [41] fuzzy fractional compartment model of coronavirus [42]. This model of a system of six equations was constructed by Khan et al. [43] in their paper involving non-linear fractional-order differential equations. The system consists of cases such as susceptible, exposed, mildly infected, asymptotically infected, recovered, and reservoir, denoted by the parameters, respectively. The asymptomatic compartment represents people who are infected with the virus but do not show any symptoms, while the mild compartment represents people who have a mild form of the disease.

The notations are classified as follows:

- η - birth rate
- ζ - a high death rate
- ξ - coefficient of transmission
- τ - coefficient of disease transmission
- ν - multiple transmissibility
- θ_1, θ_2 - represented the period of incubation.
- ϱ_1, ϱ_2 - rate of recovery
- Ξ - virus transmission from infected to reservoir
- \beth - virus transmission from asymptotically infected to reservoir
- \varkappa - the rate at which the virus is eradicated from reservoir

$$\left\{ \begin{array}{l} D_t^C S_k(t) = \eta - \zeta S_k - \tau S_k (\mathcal{J}_k + \nu \mathcal{A}_k) - \tau S_k \mathcal{M}_k \\ D_t^C \mathcal{E}_k(t) = \tau S_k (\mathcal{J}_k + \delta \mathcal{A}_k) + \xi S_k \mathcal{M} - (1 - \delta_k) \theta_1 \mathcal{E}_k - \delta_k \theta_2 \mathcal{E}_k - \zeta \mathcal{E}_k \\ D_t^C \mathcal{J}_k(t) = (1 - \delta_k) \theta \mathcal{E}_k - (\tilde{\eta} + \zeta) \mathcal{J}_k \\ D_t^C \mathcal{A}_k(t) = \delta_k \theta_1 \mathcal{E}_k - (\tilde{\eta}_1 + \zeta) \mathcal{A}_k \\ D_t^C \mathcal{R}_k(t) = \gamma_k \mathcal{J}_k + \tilde{\eta}_1 \mathcal{A}_k - \zeta \mathcal{R}_k \\ D_t^C \mathcal{M}_k(t) = \xi \mathcal{J}_k + \eta \mathcal{A}_k - \varphi \mathcal{M}_k \end{array} \right. \quad (4)$$

Correlated to uncertain initial condition, for $t \in [0, 1]$.

$$\begin{aligned} \tilde{S}(0, t) &= (\underline{S}(0, t), \bar{S}(0, t)), \\ \tilde{E}(0, t) &= (\underline{E}(0, t), \bar{E}(0, t)), \\ \tilde{I}(0, t) &= (\underline{I}(0, t), \bar{I}(0, t)), \\ \tilde{A}(0, t) &= (\underline{A}(0, t), \bar{A}(0, t)), \\ \tilde{R}(0, t) &= (\underline{R}(0, t), \bar{R}(0, t)), \\ \tilde{M}(0, t) &= (\underline{M}(0, t), \bar{M}(0, t)). \end{aligned}$$

The above-mentioned system's Simulink block diagram is shown in Figure 11.

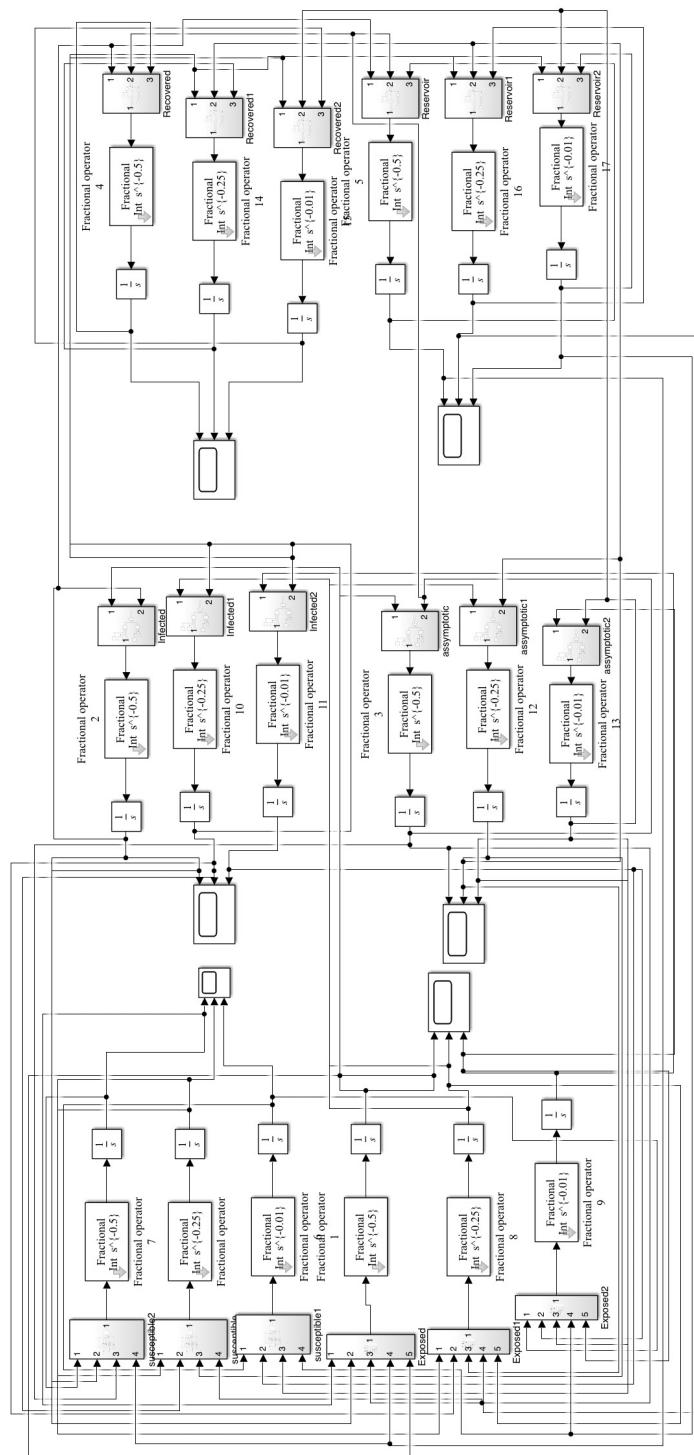


Figure 11. Block diagram of Simulink for equation (4)

The graph produced by the SEIARM model typically shows the number of individuals in each compartment over time. The susceptible, exposed, asymptomatic, mild, and infected compartments all show an increase in the number of individuals over time as the virus spreads. The recovered compartment has also increased over time as more people recover from the disease. The exposed population grows as the susceptible class value falls, and infection spreads at a varied rate due to different fractional orders, as seen in Figures 12(A), 12(B), 12(C), 12(D), 12(E), and 12(F). When the

number of death cases increases, the recovered class, as well as the asymptotically infected class, expands, and the virus population in the reservoir grows. Interpreting the graph provides us with an insight into how the disease is spreading, how many people are being infected, and how effective interventions like vaccination or social distancing measures are at slowing the spread of the disease. It can also provide projections for future trends in the spread of the disease, which can be useful for public health planning and resource allocation.

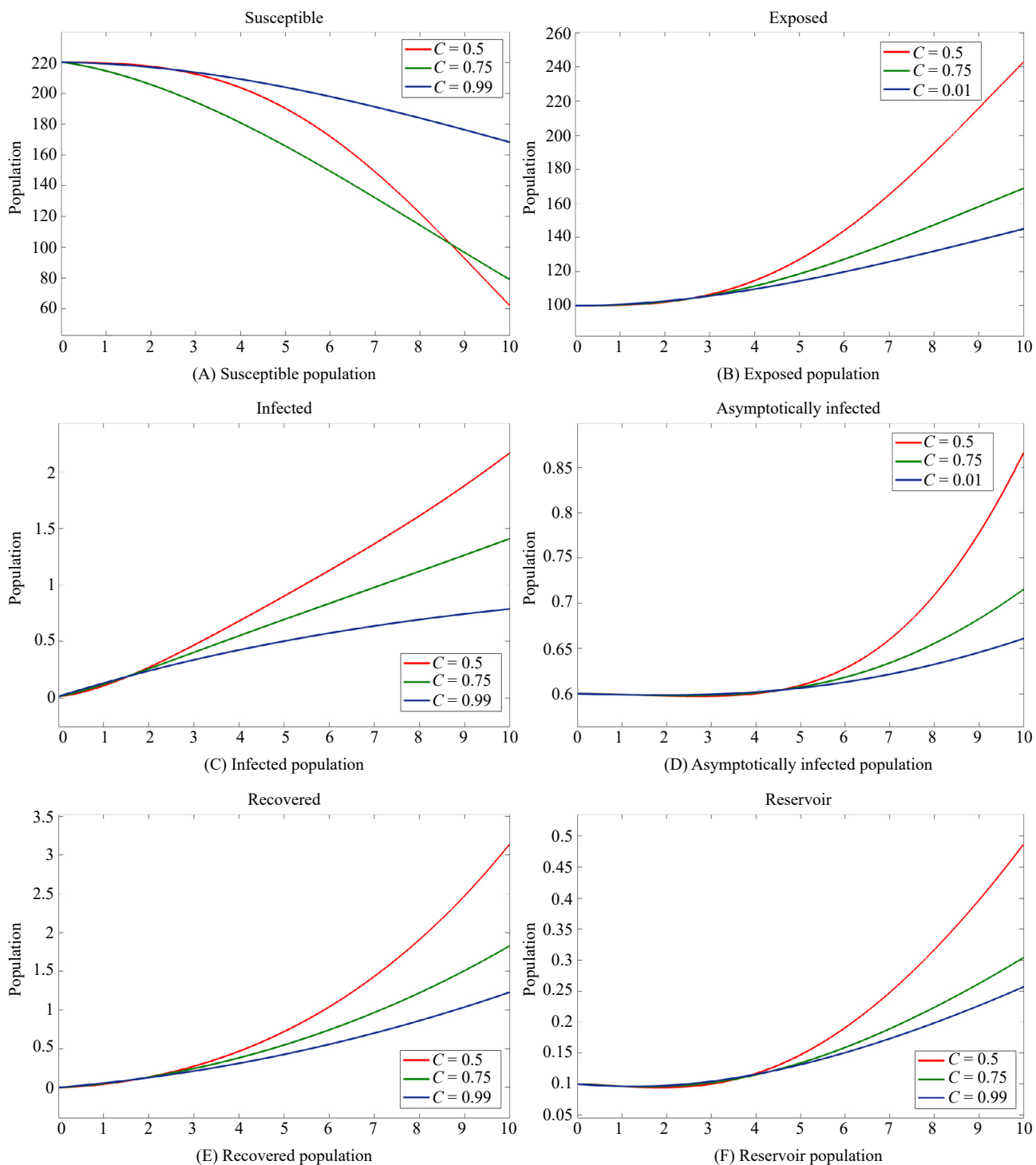


Figure 12. Dynamic behaviour of SEIARM model for $C = 0.5, 0.75, 0.99$

3.5 Simulink's academic significance

Like MATLAB coding, Simulink is another tool that helps students and researchers simulate and identify the convergence of any dynamical system, both in integer and fractional order. Hence, it becomes easy for the students to study in detail about the various epidemiology models like SIR, SEIR, and so on in a graphical way and could relate to the most happening epidemic's behaviour with a broad knowledge.

4. Conclusion

This paper dealt with analysing the various mathematical models for the COVID-19 epidemic. The model was designed based on the Caputo fractional derivative. Simulink models were used to simulate and predict the COVID-19 outbreak in this paper. The models can be used to mimic pandemic outbreaks and are simple to develop. Several models, including SIR, SIRD, SEIRD, and SEIARM, were given. The model, which has produced promising results, is implemented using the Caputo fractional derivative. In this study, it is shown that using Simulink rather than a particular approach to solve the COVID-19 fractional order model is more effective. However, the study reveals that the Simulink-based solution is efficient when compared to other similar approaches, and it might be useful in further pandemic research. The numerical simulations show that there is a good agreement between the results obtained through Simulink simulation and those obtained through MATLAB code.

Conflict of interest

There is no conflict of interest in this study.

References

- [1] World Health Organization. *Novel coronavirus (2019-nCoV): Situation report - 1*. <https://www.who.int/docs/default-source/coronaviruse/situation-reports/20200121-sitrep-1-2019-ncov.pdf> [Accessed 21st January 2020].
- [2] Kolokolnikov T, Iron D. Law of mass action and saturation in SIR model with application to coronavirus modelling. *Infectious Disease Modelling*. 2021; 6: 91-97. Available from: <https://doi.org/10.1016/j.idm.2020.11.002>.
- [3] He S, Peng Y, Sun K. SEIR modeling of the COVID-19 and its dynamics. *Nonlinear Dynamics*. 2020; 101: 1667-1680. Available from: <https://doi.org/10.1007/s11071-020-05743-y>.
- [4] Calafiore GC, Novara C, Possieri C. A time-varying SIRD model for the COVID-19 contagion in Italy. *Annual Reviews in Control*. 2020; 50: 361-372. Available from: <https://doi.org/10.1016/j.arcontrol.2020.10.005>.
- [5] Abdulrahman I. SimCOVID: Open-source simulation programs for the COVID-19 outbreak. *SN Computer Science*. 2023; 4: 20. Available from: <https://doi.org/10.1007/s42979-022-01441-1>.
- [6] Kumar S, Chauhan RP, Momani S, Hadid S. Numerical investigations on COVID-19 model through singular and non-singular fractional operators. *Numerical Methods for Partial Differential Equations*. 2024; 40(1): e22707. Available from: <https://doi.org/10.1002/num.22707>.
- [7] Toledo-Hernandez R, Rico-Ramirez V, Iglesias-Silva GA, Diwekar UM. A fractional calculus approach to the dynamic optimization of biological reactive systems. Part I: Fractional models for biological reactions. *Chemical Engineering Science*. 2014; 117: 217-228. Available from: <https://doi.org/10.1016/j.ces.2014.06.034>.
- [8] Samko S, Kilbas AA, Marichev O. *Fractional integrals and derivatives*. Taylor & Francis; 1993.
- [9] Magin R. Fractional calculus in bioengineering, part 1. *Critical ReviewsTM in Biomedical Engineering*. 2004; 32(1): 104. Available from: <https://doi.org/10.1615/CritRevBiomedEng.v32.i1.10>.
- [10] Hilfer R. (ed.) *Applications of fractional calculus in physics*. Singapore: World Scientific; 2000. Available from: <https://doi.org/10.1142/3779>.
- [11] Awawdeh F, Adawi A, Mustafa Z. Solutions of the SIR models of epidemics using HAM. *Chaos, Solitons &*

- Fractals*. 2009; 42(5): 3047-3052. Available from: <https://doi.org/10.1016/j.chaos.2009.04.012>.
- [12] Biazar J. Solution of the epidemic model by Adomian decomposition method. *Applied Mathematics and Computation*. 2006; 173(2): 1101-1106. Available from: <https://doi.org/10.1016/j.amc.2005.04.036>.
- [13] Rafei M, Ganji DD, Daniali H. Solution of the epidemic model by homotopy perturbation method. *Applied Mathematics and Computation*. 2007; 187(2): 1056-1062. Available from: <https://doi.org/10.1016/j.amc.2006.09.019>.
- [14] Khan A, Khan TS, Syam MI, Khan H. Analytical solutions of time-fractional wave equation by double Laplace transform method. *The European Physical Journal Plus*. 2019; 134: 163. Available from: <https://doi.org/10.1140/epjp/i2019-12499-y>.
- [15] Kumar S, Kumar A, Samet B, Dutta H. A study on fractional host-parasitoid population dynamical model to describe insect species. *Numerical Methods for Partial Differential Equations*. 2021; 37(2): 1673-1692. Available from: <https://doi.org/10.1002/num.22603>.
- [16] Kumar S, Kumar R, Osman MS, Samet B. A wavelet based numerical scheme for fractional order SEIR epidemic of measles by using Genocchi polynomials. *Numerical Methods for Partial Differential Equations*. 2021; 37(2): 1250-1268. Available from: <https://doi.org/10.1002/num.22577>.
- [17] Mohammadi H, Kumar S, Rezapour S, Etemad S. A theoretical study of the Caputo-Fabrizio fractional modeling for hearing loss due to Mumps virus with optimal control. *Chaos, Solitons & Fractals*. 2021; 144: 110688. Available from: <https://doi.org/10.1016/j.chaos.2021.110688>.
- [18] Kumar S, Kumar R, Cattani C, Samet B. Chaotic behaviour of fractional predator-prey dynamical system. *Chaos, Solitons & Fractals*. 2020; 135: 109811. Available from: <https://doi.org/10.1016/j.chaos.2020.109811>.
- [19] Erturk VS, Godwe E, Baleanu D, Kumar P, Asad J, Jajarmi A. Novel fractional-order Lagrangian to describe motion of beam on nanowire. *Acta Physica Polonica A*. 2021; 140(3): 265-272. Available from: <https://doi.org/10.12693/APhysPolA.140.265>.
- [20] Kumar P, Erturk VS, Yusuf A, Kumar S. Fractional time-delay mathematical modeling of oncolytic virotherapy. *Chaos, Solitons & Fractals*. 2021; 150: 111123. Available from: <https://doi.org/10.1016/j.chaos.2021.111123>.
- [21] Din A, Khan FM, Khan ZU, Yusuf A, Munir T. The mathematical study of climate change model under nonlocal fractional derivative. *Partial Differential Equations in Applied Mathematics*. 2022; 5: 100204. Available from: <https://doi.org/10.1016/j.padiff.2021.100204>.
- [22] Viera-Martin E, Gómez-Aguilar JF, Solís-Pérez JE, Hernández-Pérez JA, Escobar-Jiménez RF. Artificial neural networks: A practical review of applications involving fractional calculus. *The European Physical Journal Special Topics*. 2022; 231(10): 2059-2095. Available from: <https://doi.org/10.1140/epjs/s11734-022-00455-3>.
- [23] Yang Q, Chen D, Zhao T, Chen Y. Fractional calculus in image processing: A review. *Fractional Calculus and Applied Analysis*. 2016; 19(5): 1222-1249. Available from: <https://doi.org/10.1515/fca-2016-0063>.
- [24] Erturk VS, Ahmadvanlu A, Kumar P, Govindaraj V. Some novel mathematical analysis on a corneal shape model by using Caputo fractional derivative. *Optik*. 2022; 261: 169086. Available from: <https://doi.org/10.1016/j.ijleo.2022.169086>.
- [25] Erturk VS, Alomari AK, Kumar P, Murillo-Arcila M. Analytic solution for the strongly nonlinear multi-order fractional version of a BVP occurring in chemical reactor theory. *Discrete Dynamics in Nature and Society*. 2022; 2022: 8655340. Available from: <https://doi.org/10.1155/2022/8655340>.
- [26] Kumar P, Govindaraj V, Erturk VS, Abdellatif MH. A study on the dynamics of alkali-silica chemical reaction by using Caputo fractional derivative. *Pramana*. 2022; 96(3): 128. Available from: <https://doi.org/10.1007/s12043-022-02359-2>.
- [27] Kermack WO, McKendrick AG. Contributions to the mathematical theory of epidemics—I. *Bulletin of Mathematical Biology*. 1991; 53(1-2): 33-55. Available from: [https://doi.org/10.1016/S0092-8240\(05\)80040-0](https://doi.org/10.1016/S0092-8240(05)80040-0).
- [28] Alshomrani AS, Ullah MZ, Baleanu D. Caputo SIR model for COVID-19 under optimized fractional order. *Advances in Difference Equations*. 2021; 2021: 185. Available from: <https://doi.org/10.1186/s13662-021-03345-5>.
- [29] Shah NH, Suthar AH, Jayswal EN, Sikarwar A. Fractional SIR-model for estimating transmission dynamics of COVID-19 in India. *J — Multidisciplinary Scientific Journal*. 2021; 4(2): 86-100. Available from: <https://doi.org/10.3390/j4020008>.
- [30] Koziół K, Stanisławski R, Bialic G. Fractional-order sir epidemic model for transmission prediction of COVID-19

disease. *Applied Sciences*. 2020; 10(23): 8316. <https://doi.org/10.3390/app10238316>.

- [31] Hasan A, Susanto H, Tjahjono V, Kusdiantara R, Putri E, Nuraini N, et al. A new estimation method for COVID-19 time-varying reproduction number using active cases. *Scientific Reports*. 2022; 12: 6675. Available from: <https://doi.org/10.1038/s41598-022-10723-w>.
- [32] Nisar KS, Ahmad S, Ullah A, Shah K, Alrabaiah H, Arfan M. Mathematical analysis of SIRD model of COVID-19 with Caputo fractional derivative based on real data. *Results in Physics*. 2021; 21: 103772. Available from: <https://doi.org/10.1016/j.rinp.2020.103772>.
- [33] Mohammadi H, Rezapour S, Jajarmi A. On the fractional SIRD mathematical model and control for the transmission of COVID-19: The first and the second waves of the disease in Iran and Japan. *ISA Transactions*. 2022; 124: 103-114. Available from: <https://doi.org/10.1016/j.isatra.2021.04.012>.
- [34] Fernández-Villaverde J, Jones CI. Estimating and simulating a SIRD model of COVID-19 for many countries, states, and cities. *Journal of Economic Dynamics and Control*. 2022; 104: 104318. Available from: <https://doi.org/10.1016/j.jedc.2022.104318>.
- [35] Al-Raei M. The forecasting of COVID-19 with mortality using SIRD epidemic model for the United States, Russia, China, and the Syrian Arab Republic. *AIP Advances*. 2020; 6: 065325. Available from: <https://doi.org/10.1063/5.0014275>.
- [36] Nisar KS, Ahmad S, Ullah A, Shah K, Alrabaiah H, Arfan M. Mathematical analysis of SIRD model of COVID-19 with Caputo fractional derivative based on real data. *Results in Physics*. 2021; 21: 103772. Available from: <https://doi.org/10.1016/j.rinp.2020.103772>.
- [37] Babaei A, Ahmadi M, Jafari H, Liya A. A mathematical model to examine the effect of quarantine on the spread of coronavirus. *Chaos, Solitons & Fractals*. 2021; 142: 110418. Available from: <https://doi.org/10.1016/j.chaos.2020.110418>.
- [38] Sinan M, Ali A, Shah K, Assiri TA, Nofal TA. Stability analysis and optimal control of COVID-19 pandemic SEIQR fractional mathematical model with harmonic mean type incidence rate and treatment. *Results in Physics*. 2021; 22: 103873. Available from: <https://doi.org/10.1016/j.rinp.2021.103873>.
- [39] Hussain T, Ozair M, Ali F, ur Rehman S, Assiri TA, Mahmoud EE. Sensitivity analysis and optimal control of COVID-19 dynamics based on SEIQR model. *Results in Physics*. 2021; 22: 103956. Available from: <https://doi.org/10.1016/j.rinp.2021.103956>.
- [40] Youssef H, Alghamdi N, Ezzat MA, El-Bary AA, Shawky AM. Study on the SEIQR model and applying the epidemiological rates of COVID-19 epidemic spread in Saudi Arabia. *Infectious Disease Modelling*. 2021; 6: 678-692. Available from: <https://doi.org/10.1016/j.idm.2021.04.005>.
- [41] Panda SK. Applying fixed point methods and fractional operators in the modelling of novel coronavirus 2019-nCoV/SARS-CoV-2. *Results in Physics*. 2020; 19: 103433. Available from: <https://doi.org/10.1016/j.rinp.2020.103433>.
- [42] Ahmad S, Ullah A, Shah K, Salahshour S, Ahmadian A, Ciano T. Fuzzy fractional-order model of the novel coronavirus. *Advances in Difference Equations*. 2020; 2020: 472. Available from: <https://doi.org/10.1186/s13662-020-02934-0>.
- [43] Khan MA, Atangana A. Modeling the dynamics of novel coronavirus (2019-nCoV) with fractional derivative. *Alexandria Engineering Journal*. 2020; 59(4): 2379-2389. Available from: <https://doi.org/10.1016/j.aej.2020.02.033>.